Numerical simulations and results

1 Eigenvalue problems

We begin by fixing some notation. Let $\Omega := PQR = (0,0), (1,0), (a_1, b_1)$ be an acute triangle, with angles (α, β, γ) and PQ=1. Let $\hat{\Omega}$ denote the reference triangle $(0,0), (1,0), (0,1)$. These domains are shown in Figure 1. We denote by $F : \hat{\Omega} \to \Omega$ the affine mapping which take us from the reference triangle $\hat{\Omega}$ to $\Omega = PQR$. Concretely, we can write this in terms of a 2×2 invertible matrix B as

$$F(\hat{x}) = B\hat{x} = x \in \Omega, \qquad B := \begin{pmatrix} 1 & a_1 \\ 0 & b_1 \end{pmatrix}$$

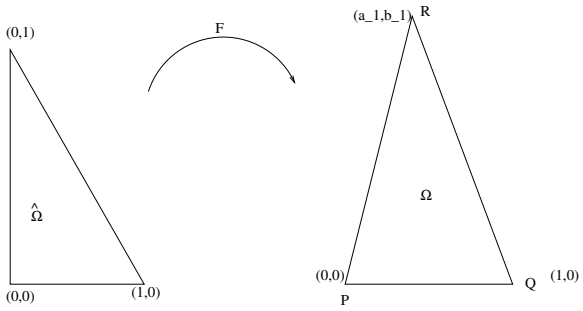

Figure 1: $\hat{\Omega}$ and the triangle $PQR = \Omega$

We'll denote by $[\cdot,\cdot], (\cdot,\cdot)$ the L^2-inner products on $\hat{\Omega}, \Omega$, respectively. We'll also need the following symmetric matrix:

$$M_1 := B^{-1}(B^{-1})^T = \frac{1}{b_1^2}\begin{pmatrix} b_1^2 + a_1^2 & -a_1 \\ -a_1 & 1 \end{pmatrix}, \tag{1}$$

$$\tag{2}$$

We now consider the following two eigenvalue problems corresponding to the 2nd Neumann eigenvalue of the Laplacian:

EVP1. *Find* $(w, \lambda_2) \in H^1(\Omega) \times \mathbb{R}^+$ *so that*

$$(\nabla w, \nabla v) = \lambda_2 (w, v) \ \forall v \in H^1(\Omega), \qquad (w,1)_1 = 0, (w,w) = 1 \tag{3a}$$

We shall denote the next Neumann eigenvalue of this problem as $\lambda_3 \geq \lambda_2$. Note that if PQR is not an equilateral triangle, $\lambda_3 > \lambda_2$.

Denoting $\hat{w} := w \circ F$, we get the following equivalent problem:

EVP2. *Find* $(\hat{w}, \hat{\lambda}_2) \in H^1(\hat{\Omega}) \times \mathbb{R}^+$ *so that*

$$[M_1 \nabla \hat{w}, \nabla v] = \hat{\lambda}_2 [\hat{w}, v] \; \forall v \in H^1(\hat{\Omega}), [\hat{w}, \hat{w}] = 1, \tag{3b}$$
$$[\hat{w}, 1] = 0 \tag{3c}$$

The spectra of the problems (EVP1), (EVP2) should be identical. That is, $\hat{\lambda}_2 = \lambda_2$.

In practice, except for special Ω, we cannot analytically compute the eigenfunctions for either (EVP1) or (EVP2). We need to employ two different kinds of approximations: a strategy for converting the infinite-dimensional eigenproblems (EVP1,EVP2) into finite-dimensional eigenproblems, and a strategy for approximating the eigenvalues of the discrete operator.

2 Numerical approximation strategy

We wish to implement a *validated* numerical strategy. The use of interval arithmetic, rather than floating point algorithms, would perhaps be optimal. However, to the best of my knowledge PDE discretization strategies have not yet been robustly implemented in interval arithmetic.

We choose a different approach. We shall be using *conforming finite elements* to discretize the eigenvalue problem6 of interest, a non-conforming method to provide lower bounds on the eigenvalues. Solutions of these are provably convergent to the true solution in exact arithmetic. These finite element approaches lead us to large, discrete generalized eigenvalue problems. The Lanczos algorithm is then used to solve these large eigenvalue problems. Both approaches have been well-studied, and their convergence properties are documented (eg. [2, 10]).We shall be performing the computations in finite-precision arithmetic.

2.1 Background: FEM approximation

Postponing for the moment the question of how to achieve this approximation, we suppose $R_h \subset H^1(\Omega)$ is a finite-dimensional subspace. We also suppose both differential and integration operators can be implemented exactly for elements in R_h. Then the discrete eigenvalue problem corresponding to (EVP1) is

DVP1. *Find* $(w_h, \lambda_{h,2}) \in (R_h \times \mathbb{R}^+) \subset (H^1(\Omega) \times \mathbb{R}^+)$ *so that*

$$(\nabla w_h, \nabla v_h) = \lambda_{h,2}(w_h, v_h) \; \forall v \in R_h \subset H^1(\Omega), (w_h, w_h) = 1 \tag{4a}$$
$$(w_h, 1) = 0 \tag{4b}$$

In practice, to maintain the same quality of approximation on all the acute triangle PQR under consideration, we may opt to use (EVP2) to calculate the eigenvalues. That is, we will be using the discrete variational formulation

DVP2. *Find* $(\hat{w}_h, \hat{\lambda}_{h,2}) \in (V_h \times \mathbb{R}^+) \subset (H^1(\hat{\Omega}) \times \mathbb{R}^+)$ *so that*

$$[M_1 \nabla \hat{w}_h, \nabla v_h] = \hat{\lambda}_{h,2} [\hat{w}_h, v_h] \; \forall v \in V_h \subset H^1(\hat{\Omega}), [\hat{w}_h, \hat{w}_h] = 1 \tag{5a}$$
$$[\hat{w}_h, 1] = 0 \tag{5b}$$

We ask: *G*iven that $\hat{\lambda}_2 = \lambda_2$, how close are $\hat{\lambda}_{h,2} = \lambda_{h,2}$? We record the quality of our approximation strategy as follows: for 3 different choices of PQR, we compute both $\hat{\lambda}_{h,2}, \lambda_{h,2}$ for several levels of refinement, and different choices of approximation spaces.

We assume $\Pi_h = \{\tau_i\}_{i=1}^T$ is a triangulation of closed triangular domain $\overline{\Omega}$, so that $\overline{\Omega} = \cup_{i=1}^T \tau_i$. Each of the triangles τ_i is called an *element*. If the triangles τ_i meet, it is either at a vertex, or along a common edge. The intersection of the interiors of elements is empty. We assume the triangulation is regular, that is,

each τ_i has an incircle of size $c_1 h$ and is contained in a circle of size $c_2 h$ where c_1, c_2 are uniform constants independent of Π_h. As the mesh parameter $h \to 0$, the number of triangles $T \to \infty$. For Π_h, we define the approximation space

$$V_h := \left\{ w \in H^1(\Omega) \middle| \; w|_{\tau_i} = \text{polynomial of degree} p, \; \forall \tau_i \in \Pi_h, \; w \text{ is continuous} \right\} \tag{6}$$

In other words, we shall primarily work with continuous conforming finite element spaces; these are often called *Lagrange elements*, [3]. It is useful to define the finite dimensional space $P_p(K) := \{v|_K : v \in V_h\}$ on a given element K. We're working with $P_p(K) =$ the set of polynomials in (x, y) of maximal degree p. A function in P_p can be uniquely determined by its values on suitably chosen points in the element K. There are canonical choices of these points, and the corresponding induced linear functionals on P_p are called the *degrees of freedom* of the element. For $P_1(K)$ the degrees of freedom at the values of the function at the three vertices of the element K; for $P_2(K)$ the degrees of freedom are given in terms of the values at the three vertices and the midpoints of the edges of K.

Since the eigenfunction of interest is not analytic up to the boundary, we cannot expect to use arbitrarily high-degree polynomials p in our approximation. The best approximation error of $u \in H^k(\Omega)$ by functions in a conforming finite element space of piecewise polynomials of degree p and mesh parameter h is known to be (eg., [8, 10])

$$\inf_{w \in V_h} \|u - w\|_{1,2} \leq C(p) h^{\mu - 1} \|u\|_{H^k(\Omega)}, \qquad \mu = \min(k, p+1).$$

In other words, we cannot hope to choose an arbitrarily high p.

For example, if $p = 1$, the optimal error estimate (ie, the error of the Ritz projection R_h) is

$$\|u - R_h u\|_{k,2} \leq c h^{2-k} \|u\|_{2,2}, k = 0, 1.$$

In other words, the best approximation in the L^2 norm by piecewise linears goes as Ch^2; the H^1 error only decreases as ch. We also record the sup-norm error estimate

$$\|u - R_h u\|_{k,\infty} \leq c h^{2-k} \log(1/h) \|u\|_{2,\infty}, k = 0, 1.$$

Since the discrete eigenvalues satisfy a relation of the form $\lambda_h = \|\nabla u_h\|^2$ (if we normalize $\|u_h\|_{0,2} = 1$), we can expect

$$|\lambda - \lambda_h| \leq C(p) h^{2\mu - 2} \|u\|_{H^k(\Omega)}, \qquad \mu = \min(k, p+1). \tag{7}$$

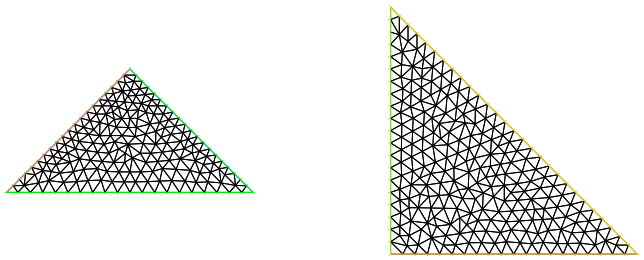

Figure 2: Left: tesselation of $\Omega = PQR$. Right: tesselation of reference triangle $\hat{\Omega}$

On a triangle, in the neighbourhood of an angle α, the eigenfunctions are known to be asymptotically $\sim r^{\frac{\pi}{\alpha}}$. We are on an acute triangle, so $0 < \alpha < \frac{\pi}{2}$, and therefore $\frac{\pi}{\alpha} > 2$. As mentioned in the notes on `http://michaelnielsen.org/polymath1/index.php?title=The_hot_spots_conjecture#Regularity_theory`, the third derivatives blow up as $O(|x - x_0|^{-1+\epsilon})$ near a corner x_0, and therefore the eigenfunctions will be in $H^3(\Omega)$, but no better. This means that we cannot expect the eigenfunctions to converge better than quadratically in the 1-norm. Nor is there much point in using better than piecewise quadratics.

It is easy to see that since V_h is a finite-dimensional subspace of $H^1(\Omega)$. Moreover, since the numerically computed eigenvalues $\lambda_{k,h}$ are minimizers (over the appropriately constrained subspace) of the Rayleigh-Ritz quotient, we see $\lambda_{k,h} \geq \lambda_k$ for all $k = 1, 2, ...$ We are guaranteed that the numerically approximated eigenfunctions are in the same spaces as the true eigenfunction.

In practice, we cannot actually compute an infinite sequence of these approximations. We can only refine the triangulation Π_h a finite number of times, and so we only obtain a finite collection $\{\lambda_{k,h_i}\}_{i=1}^M$ of approximations to λ_k. We know that if $h_1 > h_2 > h_3 ... > h_M$, then $\lambda_k \leq \lambda_{k,h_M} \leq \lambda_{k,h_{M-1}} ....$ Knowledge of λ_{k,h_M} alone does not tell us how close we are to λ_k.

How close are we to the actual eigenvalue? One way to answer this question is to use a different kind of convergent discretization which will produce a finite collection $\{\tilde{\lambda}_{k,h_i}\}_{i=1}^M$ of approximations to λ_k, where if $h_1 > h_2 > h_3 ... > h_M$, then $\lambda_k \geq \tilde{\lambda}_{k,h_M} \geq \tilde{\lambda}_{k,h_{M-1}} ....$ We now have the relation

$$\tilde{\lambda}_{k,h_M} \leq \lambda_k \leq \lambda_{k,h_M}.$$

The quantities on the right and left are computable, and we are guaranteed that the true eigenvalue is contained in the interval between them.

A discretization strategy which provides eigenvalue bounds from below is given by using certain *non-conforming finite element methods*. Here the approximation space W_h is not a strict subspace of $H^1(\Omega)$. This methodology is described in [1, 11]. In these papers, the key results are proved for the Dirichlet eigenvalue problems. The Dirichlet datum is only used to invoke the Poincaré inequality in the proofs. Since we are interested in mean-zero eigenfunctions for the Neumann eigenproblem, the results from these papers still hold. The only change is to work with the equivalent but shifted eigenvalue problem $(\nabla w, \nabla v) + (w, v) = (1 + \lambda_2)(w, v),\ \forall v \in H^1(\Omega), (w, 1) = 0$.

Following [11], we use piecewise-linear Crouzeix-Raviert non-conforming finite element to get lower bounds on the eigenvalue. These finite element spaces are comprised of piecewise linear polynomials with degrees of freedom at the midpoints of the edges of elements. We use a piece-wise linear conforming Lagrange elements to give us upper bounds on the eigenvalues. Putting these together gives us an *interval* around the true eigenvalue.

2.2 Background: Eigenfunction approximation

Using the methods in Section 2.1, we are lead to a finite-dimensional eigenvalue problem, (5a). Let us denote the size of the system as N. The properties of the approximations as $N \to \infty$ is discussed in the previous section. For the purposes of this section, we fix N.

Let $\{\phi_i\}_{i=1}^N$ be a basis for our approximation space $V_h \subset H^1(\hat{\Omega})$. We have

$$\hat{w}_2 \approx \hat{w}_{2,h} = \sum_{i=1}^{N} u_i \phi_i,$$

where the coefficients $\vec{u}_h = (u_1, u_2, ..., u_N)^T$ are determined by solving the generalized eigenvalue problem

$$\mathrm{A}_N \vec{u}_h = \lambda_{h,2} \mathrm{B}_N \vec{u}_h \text{ where} \tag{8}$$

$$(\mathrm{A}_N)_{ij} = (M_1 \nabla \phi_i, \nabla \phi_j), \qquad (\mathrm{B}_N)_{ij} = (\phi_j, \phi_j)\ \forall j = 1, 2....N. \tag{9}$$

For the conforming finite element method, this is a large, symmetric and sparse generalized eigenvalue problem. and will be solved using the Lanczos iteration, [4, 9, 6]. The specific implementation we use is from `ARPACK`.

We have two levels of approximation to consider. The Lanczos method is iterative, and if we implemented it in exact arithmetic, we would need to examine the properties of the iterates. In practice, we are implementing this algorithm in finite precision, and so we need to be concerned with the effects of rounding. These issues have been studied in detail in, for example, [6, 7].

We present an analysis which is suitable for simple eigenvalues, which is described in more detail in the notes edited by Bai, Demmel, Dongarra, Ruhe and van der Vorst in `http://web.eecs.utk.edu/ dongarra/etemplates/book` in the section on Hermitian eigenvalue problems.

Suppose we compute the eigenpair $(\tilde{u}, \tilde{\lambda})$ to approximate the actual eigenpair $(\vec{u}_h, \lambda_{h,2}$ for the system above. In this case,

$$A_N \tilde{u} = \tilde{\lambda} B_N \tilde{u} + r.$$

Since the Lanczos algorithm is backward stable, and both A_N, B_N are real and symmetric, there are real symmetric matrices E such that

$$(A_N + E)\tilde{u} = \tilde{\lambda} B_N \tilde{u}.$$

One such E is given by

$$E = -r\tilde{u}^T - \tilde{u}r^T + (\tilde{u}^T A_N \tilde{u} - \tilde{\lambda}\tilde{u}^T B_N \tilde{u}),$$

with the matrix 2-norm of E given by $\|E\|_2 = \|r\|_2$. If r is small in norm, then it can be shown that

$$|\tilde{\lambda} - \lambda_{h,2}| \leq \frac{\|r\|_2^2}{\delta}, \qquad \delta := \min_{k \neq 2} |\tilde{\lambda} - \lambda_{h,k}|.$$

Here δ is the distance of $\tilde{\lambda}$ from the other true eigenvalues. We can get reasonable bounds distance for our problem, since we know $\lambda_{h,1} = 0$ and have an approximation for $\lambda_{h,3}$. We also have that the solid angle θ between the computed eigenvector $\tilde{u}$ and the actual eigenvector $\vec{u}_h$ satisfies

$$\sin(\theta) \leq \frac{\|r\|_2}{\delta}.$$

In practice, we keep track of several measures of error. We record the residual vector $r := A_N \tilde{u} - \tilde{\lambda} B_N \tilde{u}$, and compute $\|r\|_{2,h} := \frac{\|r\|_2}{N}$. Here $\|r\|_2$ is the vector 2-norm of the residual vector and N is the size of the matrix. We record the bounds $\frac{\|r\|_{2,h}^2}{\delta}$ and $\frac{\|r\|_2}{\delta}$. We also compute the residual of the Ritz quotient,$[M_1 \nabla\hat{w}, \nabla\hat{w}] - \hat{\lambda}[\hat{w}, \hat{w}]$.

2.3 Location of extrema

Once we have computed the discrete eigenfunction $\hat{w}_h$ approximating the 2nd Neumann eigenfunction for (5a), we still need to locate its extremum. Since we will use P_2 conforming elements to compute $\hat{w}_h$, the discrete eigenfunction is piecewise quadratic; the degrees of freedom (values on nodes) are not guaranteed to be extrema. If we locate the extrema on nodes, these are not guaranteed to converge to the location of the true extremum either.

In order to numerically locate the extrema of $\hat{w}_h$, we first compute its interpolant $\mathcal{I}_F \hat{w}_h$ from the approximation space

$$V_F := \left\{ w \in H^1(\hat{\Omega}) | w|_{\tau_i} = \text{polynomial of degree } 1, \forall \tau_i \in \Pi_F,\ w \text{ is continuous} \right\}. \tag{10}$$

Here $F >> M$ corresponds to a very fine tesselation of $\hat{\Omega}$. The extremum of the nodal values of $\mathcal{I}_F \hat{w}_h$ will correspond to the extremum of $\mathcal{I}_F \hat{w}_h$ (because the interpolant is piecewise linear). We therefore perform a simple search for the extrema on the nodes of this interpolant.

3 Calculation of bound

The strategies outlined in Sections 2.1 and 2.2 describe how to find the approximate eigenfunction for *one* point $(\alpha_i, \beta_i, \gamma_i)$ in angle-parameter space. However, we need to perform these computations for *several* such points. In the vicinity of each such point, we will employ perturbative arguments to conclude that the eigenfunctions of a triangle $(\alpha_i + \delta_a, \beta_i + \delta_b, \gamma_i + \delta_c)$ are 'close' to those corresponding to $(\alpha_i, \beta_i, \gamma_i)$.

What do we mean by 'close'? We are interested in the location of the extrema of the second eigenfunction, so we need to control sup norm of the variation. That is, if we specify a tolerance ϵ, we wish to estimate the neighbourhood of $(\alpha_i, \beta_i, \gamma_i)$ so that information about the eigenfunction for this triangle gives a good indication for the eigenfunctions of other triangles in the neighbourhood. These calculations have been done in

`http://terrytao.files.wordpress.com/2012/07/perturbation1.pdf.`

Given a desired tolerance ϵ, we need to compute the permissable size of δ_a, δ_b by using the RHS of the bounds in

`http://terrytao.files.wordpress.com/2012/07/perturbation1.pdf`

We want to find δ so that if the angles are linearly perturbed by this amount then

$$X = \frac{4}{3\min(\sin(\alpha), \sin(\beta), \sin(\gamma)} |ABC|^{1/2} \frac{2\lambda_2\lambda_3}{\lambda_3 - \lambda_2} \left(\int_{\mathbb{H}} |\dot{\omega}|^2 e^{2\omega} \right)^{1/2} < \epsilon$$

Since the numerical computations are done on a triangle PQR which is similar to ABC, with $|PQ| = 1$ we have to rewrite X on PQR. Denoting by $\tilde{\lambda_i}$ the eigenvalues on PQR, we get the scalings

$$\tilde{\lambda_i} = |AB|^2 \lambda_i, |ABC| = |AB|^2 |PQR|,$$

and therefore

$$X = \frac{4}{3\min(\sin(\alpha), \sin(\beta), \sin(\gamma)} |PQR|^{1/2} \frac{\tilde{\lambda_2}\tilde{\lambda_3}}{|AB|(\tilde{\lambda_3} - \tilde{\lambda_2})} \left(\int_{4\mathbb{H}} |\dot{\omega}|^2 e^{2\omega} \right)^{1/2}$$

We have, for linear variations in the angles,

$$\begin{aligned} 4 \int_{\mathbb{H}} |\dot{\omega}|^2 e^{2\omega} &= \frac{d^2}{dt^2} |ABC| \\ &= \left(\dot{\alpha}^2 \frac{\partial^2}{\partial \alpha^2} + \dot{\beta}^2 \frac{\partial^2}{\partial \beta^2} + \dot{\gamma}^2 \frac{\partial^2}{\partial \gamma^2} + 2\dot{\alpha}\dot{\beta} \frac{\partial^2}{\partial \alpha \beta} + 2\dot{\alpha}\dot{\gamma} \frac{\partial^2}{\partial \alpha \gamma} + 2\dot{\beta}\dot{\gamma} \frac{\partial^2}{\partial \beta \gamma} \right) F(\alpha, \beta, \gamma) \end{aligned}$$

where

$$F(\alpha, \beta, \gamma) := |ABC| = \frac{1}{2\pi^2} \Gamma(\frac{\alpha}{\pi})^2 \Gamma(\frac{\beta}{\pi})^2 \Gamma(\frac{\gamma}{\pi})^2 \sin(\alpha)\sin(\beta)\sin(\gamma). \tag{11}$$

We shall consider two specific cases: where $\alpha(t) := \alpha + \delta t, \gamma(t) = \gamma - \delta t, \beta(t) = \beta$ and the other situation where α does not vary, but β does. This is so we can compute the spacing for sampling required in parameter space. The mesh can vary in two perpendicular directions.

We proceed to compute:

$$\begin{aligned} \log(F(\alpha, \beta, \gamma) &= 2\log(\Gamma(\frac{\alpha}{\pi})) + 2\log(\Gamma(\frac{\beta}{\pi})) + 2\log(\Gamma(\frac{\gamma}{\pi})) + \log(\sin(\alpha)) + \log(\sin(\beta)) + \log(\sin(\gamma)) - \log(2\pi^2) \\ \Rightarrow \frac{\partial}{\partial \alpha} F(\alpha, \beta, \gamma) &= F \left\{ \frac{2}{\pi} \Psi(\frac{\alpha}{\pi}) + \cot(\alpha) \right\} \\ \Rightarrow \frac{\partial^2}{\partial \alpha^2} F(\alpha, \beta, \gamma) &= F \left\{ \frac{2}{\pi^2} \Psi(1, \frac{\alpha}{\pi}) - \csc^2(\alpha) \right\} + \frac{\partial}{\partial \alpha} F(\alpha, \beta, \gamma) \left\{ \frac{2}{\pi} \Psi(\frac{\alpha}{\pi}) + \cot(\alpha) \right\} \\ &= F \left\{ \frac{2}{\pi^2} \Psi(1, \frac{\alpha}{\pi}) - \csc^2(\alpha) \right\} + F \left\{ \frac{2}{\pi} \Psi(\frac{\alpha}{\pi}) + \cot(\alpha) \right\}^2 \end{aligned}$$

where $\Psi(x)$ is the digamma function, and $\Psi(1, x)$ is the trigamma function.

Also,

$$\begin{aligned}\frac{\partial^2}{\partial\gamma\alpha}F(\alpha,\beta,\gamma) &= \frac{\partial}{\partial\gamma}F(\alpha,\beta,\gamma)\left\{\frac{2}{\pi}\Psi(\frac{\alpha}{\pi})+\cot(\alpha)\right\}\\ &= F\left\{\frac{2}{\pi}\Psi(\frac{\gamma}{\pi})+\cot(\gamma)\right\}\left\{\frac{2}{\pi}\Psi(\frac{\alpha}{\pi})+\cot(\alpha)\right\}\end{aligned}$$

Therefore

$$\begin{aligned}4\int_{\mathbb{H}}|\dot{\omega}|^2e^{2\omega} &= \left(\dot{\alpha}^2\frac{\partial^2}{\partial\alpha^2}+\dot{\gamma}^2\frac{\partial^2}{\partial\gamma^2}+2\dot{\alpha}\dot{\gamma}\frac{\partial^2}{\partial\alpha\gamma}\right)F(\alpha,\beta,\gamma)\\ &= \delta^2\left(\frac{\partial^2}{\partial\alpha^2}+\frac{\partial^2}{\partial\gamma^2}-2\frac{\partial^2}{\partial\alpha\gamma}\right)F(\alpha,\beta,\gamma)\\ &= \delta^2F(\alpha,\beta,\gamma)\left\{\frac{2}{\pi^2}\Psi(1,\frac{\alpha}{\pi})-\csc^2(\alpha)+\left(\frac{2}{\pi}\Psi(\frac{\alpha}{\pi})+\cot(\alpha)\right)^2\right.\\ &\quad+\frac{2}{\pi^2}\Psi(1,\frac{\gamma}{\pi})-\csc^2(\gamma)+\left(\frac{2}{\pi}\Psi(\frac{\gamma}{\pi})+\cot(\gamma)\right)^2\\ &\quad\left.-2\left(\frac{2}{\pi}\Psi(\frac{\gamma}{\pi})+\cot(\gamma)\right)\left(\frac{2}{\pi}\Psi(\frac{\alpha}{\pi})+\cot(\alpha)\right)\right\}\end{aligned}$$

We can write this efficiently as

$$\begin{aligned}4\int_{\mathbb{H}}|\dot{\omega}|^2e^{2\omega} &= |ABC|\delta^2\left\{G'(\alpha)+G'(\gamma)+(G(\alpha)-G(\gamma))^2\right\}\\ &= |AB|^2|PQR||\delta^2\left\{G'(\alpha)+G'(\gamma)+(G(\alpha)-G(\gamma))^2\right\}\end{aligned}$$

with $G(x) := \frac{2}{\pi}\Psi(\frac{x}{\pi})+\cot(x)$.

Putting this into the previously simplified expression for X, we get

$$X = \frac{4}{3\min(\sin(\alpha),\sin(\beta),\sin(\gamma))}|PQR|\frac{\tilde{\lambda_2}\tilde{\lambda_3}}{(\tilde{\lambda_3}-\tilde{\lambda_2})}\delta\left\{G'(\alpha)+G'(\gamma)+(G(\alpha)-G(\gamma))^2\right\}^{1/2}$$

Therefore, to ensure $X<\epsilon$,

$$\delta<\epsilon\left[\frac{4}{3\min(\sin(\alpha),\sin(\beta),\sin(\gamma))}|PQR|\frac{\tilde{\lambda_2}\tilde{\lambda_3}}{(\tilde{\lambda_3}-\tilde{\lambda_2})}\left\{G'(\alpha)+G'(\gamma)+(G(\alpha)-G(\gamma))^2\right\}^{1/2}\right]^{-1} \tag{12}$$

3.1 Overall Approximation strategy

In the pseudocode below, we describe how to numerically verify the Hot Spot conjecture for a discrete subset of points in angle-parameter space.

1: Mesh parameter space of interest (α,β,γ), ie, construct subset $\{(\alpha_i,\beta_i,\gamma_i)\}_{i=1}^N$ based on bounds computed in section 3
2: **for** $i=1\leftarrow N$ **do**
3: **procedure** CHECK HOTSPOT CONJECTURE ON PQR(angles $(\alpha_i,\beta_i,\gamma_i)$)
4: **procedure** APPROXIMATE 2ND NEUMANN EIGENFUNCTION ON PQR
5: Pull back the eigenvalue problem to the reference triangle $\hat{\Omega}$
6: Initialize mesh size h_1, set $n=0$.
7: **while** $n<M$ and $tol>1e-7$ **do**

$n \leftarrow n+1$, corresponding to near-halving of mesh size.
Triangulate $\hat{\Omega}$ with Π_{h_n}, mesh size h_n;
Compute $\hat{\lambda}_{2,h_n}, \hat{\lambda}_{3,h_n}$ by Lanczos iteration with shift =1, using P_2 conforming elements;
Compute $\tilde{\lambda}_{2,h_n}, \tilde{\lambda}_{3,h_n}, \tilde{\lambda}_{2,h_{n+1}}$ using the Lanczos iteration with shift=1, using P_1 non-conforming elements.
Compute

$$tol = \max\left\{ |\hat{\lambda}_{2,h_{n-1}} - \hat{\lambda}_{2,h_n}|, |\tilde{\lambda}_{2,h_n} - \hat{\lambda}_{2,h_n}|, |[M_1 \nabla \hat{w}_h, \nabla \hat{w}_h] - \hat{\lambda}_{h,2}[\hat{w}_h, \hat{w}_h]|, \frac{\|r\|^2_{2,h}}{\delta}, \hat{\lambda}_{h,2} \right\}$$

procedure LOCATE EXTREMA OF 2ND NEUMANN EIGENFUNCTION ON PQR($\hat{w}_{2,h_n}$)
Interpolate the numerical eigenfunction $\hat{w}_{2,h_n}$ onto P_1 approximation space with h_{2M}.
Search the grid nodal values for the extrema, and record their location;
Compute the values of the bounds described in Section 3, setting $\delta = 0.0001$.

4 Validation experiments

4.1 Validation: eigenvalue calculations on $\hat{\Omega}$ compared to those on Ω

4.1.1 Experiment 1: Equilateral triangle

This is a challenging situation because of the repeated eigenvalue. We use the calculations in [5] to obtain the first 4 exact eigenvalues on the equilateral triangle with base of length 1. The exact eigenvalues are: $0, \frac{4}{27}(2\pi\sqrt{(}3))^2, \frac{4}{27}(2\pi\sqrt{(}3))^2, \frac{4}{9s}(2\pi\sqrt{(}3))^2$. The parameters for the Arnoldi eigenvalue were set as $tolerance = 1e-30$, maximum number of iterations =30.

The computed coordinated of vertex R are $a_1 = 0.5, b_1 = 0.866025$. Recall that $\hat{\Omega}$ is the reference right triangle. We also compare the eigenvalue calculations performed with a conforming method, to those performed with a non-conforming method.

The figures in the top row of 3 and 4 show, graphically, some results for the experiments on the equilateral triangle. In the left plot of Figure 3a, we plot the error $|\lambda_{2,h} - \lambda_2|$ in the computed 2nd Neumann eigenvalue λ_2, for several different methods. As the number of vertices in our tesselation of the domain increases, the mesh size h decreases. From the figure we see clearly that using P1 finite element strategies yields second order convergence for the eigenvalue, while the eigenvalues computed with the P2 conforming strategy converge at 4th order. Also visible here is the behaviour of the P3 (cubic conforming)- the error initially appears to decrease as the number of vertices decreases, but increases again. This is consistent with the theoretical predictions of the behaviour of this method.

In the right graph of figure 3a, we see the effect of computing the 2nd second eigenvalue using the (isospectral problems) (DVP1) and (DVP2). We see that while the error in the computed eigenvalues is larger if we use a FEM method on the reference triangle, the computed eigenvalues still converge to the correct ones at the same rates.

In the left graph of figure 4a, we present the computed eigenvalues on the actual domain PQR as well as the reference domain, using the P1 and P2 conforming methods, and a suitable P1 non-conforming method (Crouzeiux-Raviert elements). One can clearly see that the computed eigenvalues using conforming and this non-conforming method approach the true value from opposite sides. For each mesh size h, one can therefore use the P1 conforming and non-conforming methods to get an interval, within which the true eigenvalue must lie. As h decreases, this interval will become smaller. In the middle and right plots of 4a, we show how close the computed eigenvalues and eigenvectors of the discrete system (8) are to the exact eigenpair for this system. This describes the behaviour of the linear algebra computations. We do not predict a particular relationship between the size of the system N and the quality of the linear algebra calculation for this system size. All we need is that as the system size N increases, the computed eigenvectors are still well-approximated by the Lanczos method.

We notice both $\frac{\|r\|_{2,h}^2}{\delta}$ and $\frac{\|r\|_2}{\delta}$ do not behave in a monotone fashion as h decreases. However, for small enough h, the angle between the computed eigenvector $\tilde{u}$ and the true eigenvector fo the discrete system $\vec{u}$ is within $asin(1e-3)$.

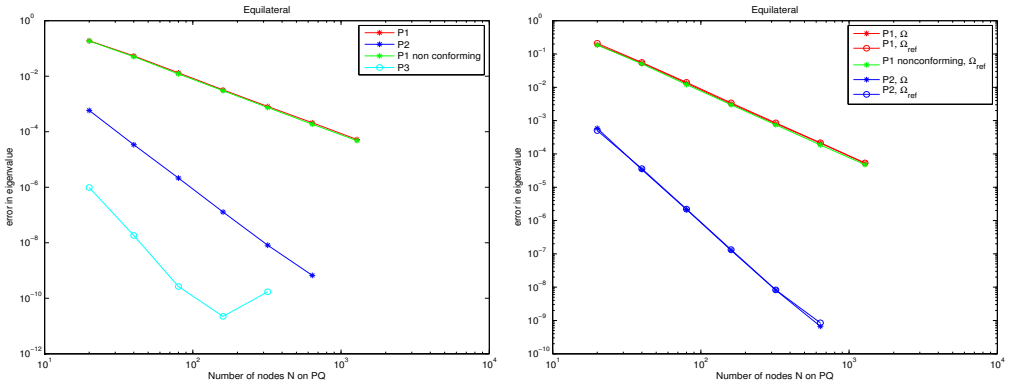

(a) Equilateral

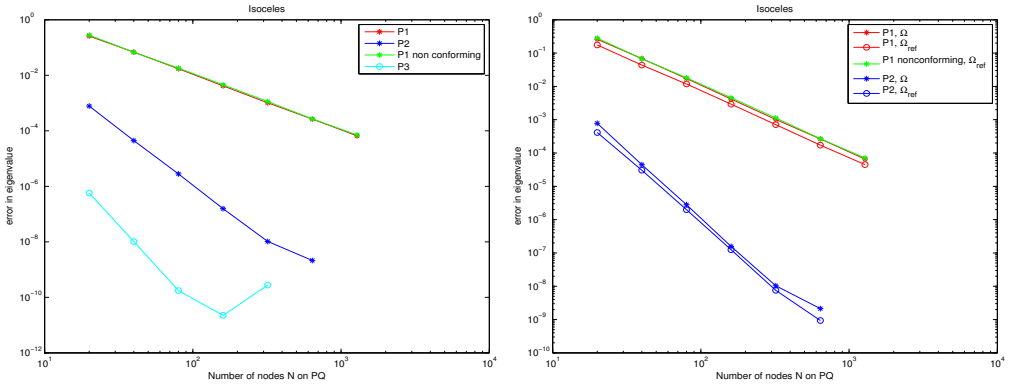

(b) Isoceles

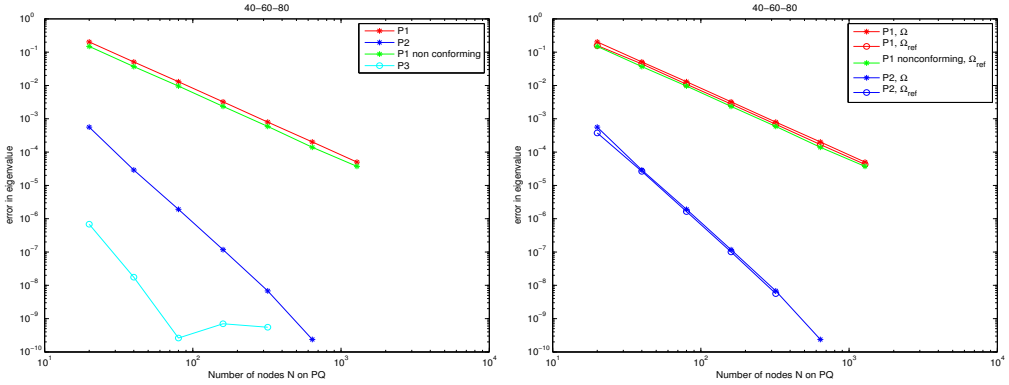

(c) 40-60-80

Figure 3: Left column: Error $|\hat{\lambda}_{h,2} - \lambda_2|$ using FEM of polynomial orders 1, 2 and 3 on $\hat{\Omega}$. Right column: Error $|\hat{\lambda}_{h,2} - \lambda_2|$ using FEM of polynomial orders 1, 2 on $\hat{\Omega}$ or Ω. In each figure, the x-axis is the number of nodes on one edge of the domain Ω.

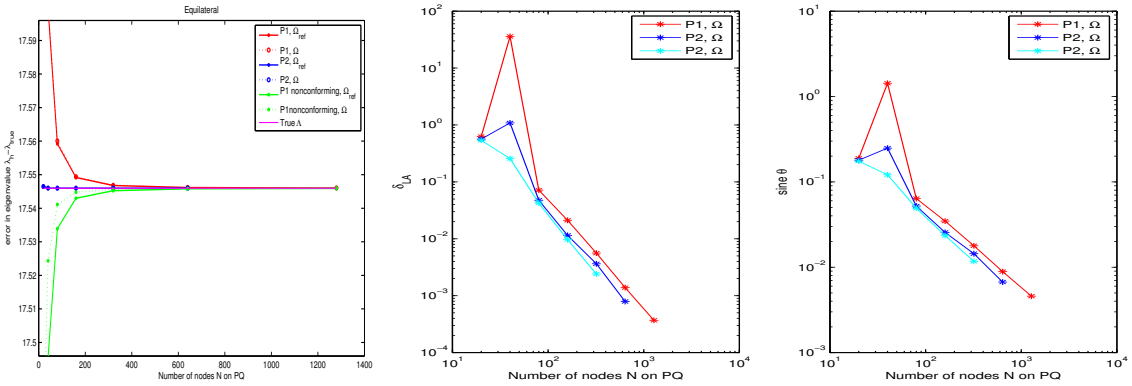

(a) Equilateral

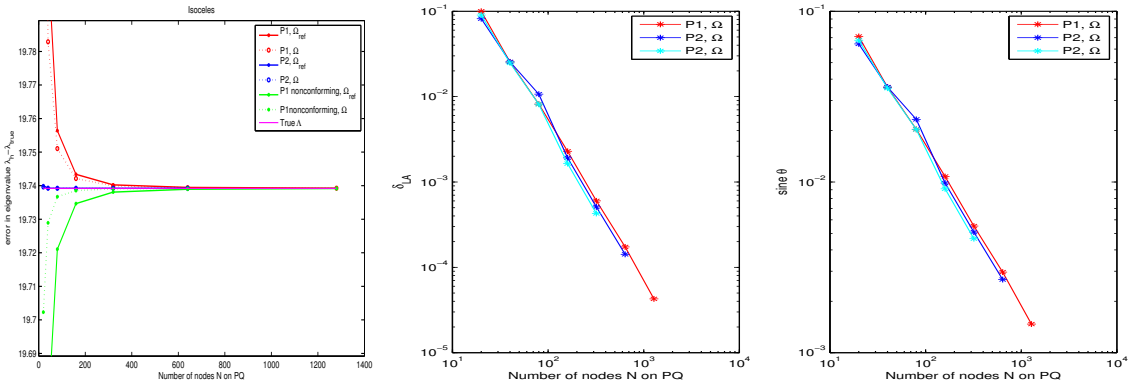

(b) Isoceles

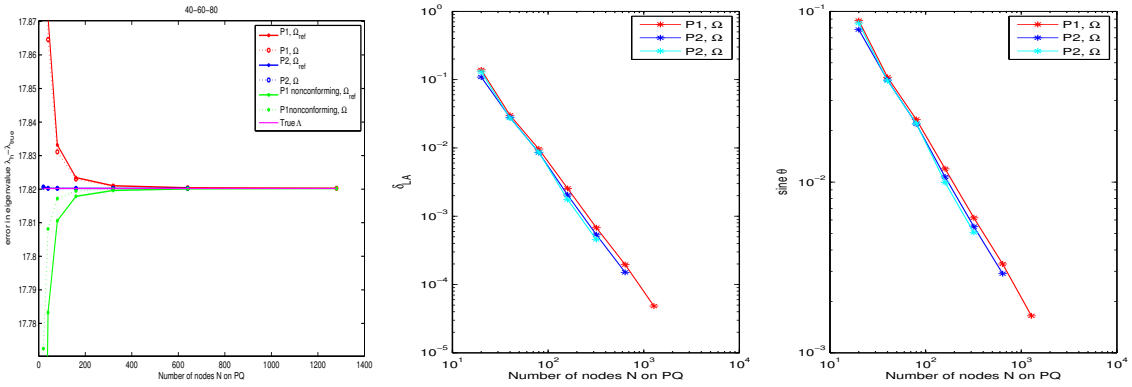

(c) 40-60-80

Figure 4: Left column: Computed $|\hat{\lambda}_{h,2}|$ using FEM of polynomial orders 1 and 2 on $\hat{\Omega}, \Omega$. Middle column: $\frac{||r||_2^2}{\delta}$ Right column: $\frac{||r||_2}{\delta}$ using FEM of polynomial orders 1, 2 on $\hat{\Omega}$.

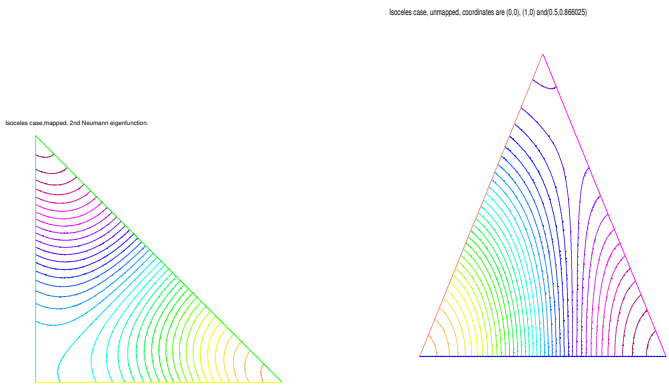

Figure 5: L: 2nd eigenfunction of EVP2 corresponding to equilateral triangle. R: 2nd eigenfunction of EVP1 on equilateral triangle

# N	$\hat{\lambda}_{h,1}$	$\hat{\lambda}_{h,1} - \lambda_1$	$\hat{\lambda}_{h,2}$	$\hat{\lambda}_{h,2} - \lambda_2$	$\hat{\lambda}_{h,3}$	$\hat{\lambda}_{h,3} - \lambda_3$	$\hat{\lambda}_{h,4}$	$\hat{\lambda}_{h,4} - \lambda_4$
10	-1.11022e-15	-1.11022e-15	17.7584	0.212412	17.7983	0.252289	54.5624	1.92455
20	-7.4607e-14	-7.4607e-14	17.5971	0.0511479	17.6142	0.0682402	53.1326	0.49472
40	-4.57412e-14	-4.57412e-14	17.5593	0.0133706	17.564	0.0179941	52.7709	0.13302
80	3.88578e-14	3.88578e-14	17.5492	0.00320021	17.5501	0.00413309	52.6686	0.0307161
160	1.58984e-12	1.58984e-12	17.5468	0.000814864	17.547	0.0010433	52.6456	0.00775507
320	2.25793e-11	2.25793e-11	17.5462	0.000209811	17.5462	0.000269075	52.6399	0.00201349

(a) P1 conforming on $\hat{\Omega}$

# N	$\hat{\lambda}_{h,1}$	$\hat{\lambda}_{h,1} - \lambda_1$	$\hat{\lambda}_{h,2}$	$\hat{\lambda}_{h,2} - \lambda_2$	$\hat{\lambda}_{h,3}$	$\hat{\lambda}_{h,3} - \lambda_3$	$\hat{\lambda}_{h,4}$	$\hat{\lambda}_{h,4} - \lambda_4$
10	-1.79856e-14	-1.79856e-14	17.7678	0.221825	17.7852	0.239231	54.7052	2.0673
20	4.55191e-14	4.55191e-14	17.6019	0.055956	17.6027	0.0567089	53.1228	0.484948
40	3.53051e-14	3.53051e-14	17.56	0.0140447	17.5604	0.0144399	52.7633	0.125437
80	2.53353e-13	2.53353e-13	17.5494	0.00345541	17.5494	0.00348365	52.6686	0.0306636
160	1.21214e-12	1.21214e-12	17.5468	0.000850507	17.5468	0.000868165	52.6456	0.00774628
320	2.4436e-11	2.4436e-11	17.5462	0.000217574	17.5462	0.000219047	52.6398	0.00194876

(b) P1 conforming on Ω

# N	$\hat{\lambda}_{h,1}$
10	6.66134e-14
20	-3.4861e-14
40	2.2804e-13
80	1.00453e-12
160	1.6116e-11
320	1.67649e-10

# N	$\hat{\lambda}_{h,1}$	$\hat{\lambda}_{h,1} - \lambda_1$	$\hat{\lambda}_{h,2}$	$\hat{\lambda}_{h,2} - \lambda_2$	$\hat{\lambda}_{h,3}$	$\hat{\lambda}_{h,3} - \lambda_3$	$\hat{\lambda}_{h,4}$	$\hat{\lambda}_{h,4} - \lambda_4$
10	-4.59632e-14	-4.59632e-14	17.4559	-0.0900435	17.4703	-0.0756578	51.9806	-0.657281
20	-2.13163e-14	-2.13163e-14	17.5253	-0.0206503	17.5267	-0.0192788	52.4762	-0.161644
40	9.88098e-14	9.88098e-14	17.5407	-0.0052285	17.541	-0.0049881	52.5956	-0.0423326
80	-1.51257e-12	-1.51257e-12	17.5448	-0.00118791	17.5448	-0.00117574	52.628	-0.00988707
160	1.08109e-11	1.08109e-11	17.5457	-0.00030156	17.5457	-0.00029722	52.6354	-0.00247977
320	1.28036e-10	1.28036e-10	17.5459	-7.57265e-05	17.5459	-7.47955e-05	52.6373	-0.000638638

(d) P1 nonconforming on Ω

Table 1: Eigenvalues using P1 conforming (a,b) and P1 non-conforming (c,d) elements on Equilateral

# N	$\hat{\lambda}_{h,1}$	$\hat{\lambda}_{h,1} - \lambda_1$	$\hat{\lambda}_{h,2}$	$\hat{\lambda}_{h,2} - \lambda_2$	$\hat{\lambda}_{h,3}$	$\hat{\lambda}_{h,3} - \lambda_3$	$\hat{\lambda}_{h,4}$	$\hat{\lambda}_{h,4} - \lambda_4$
10	3.77476e-14	3.77476e-14	17.5465	0.000496081	17.5468	0.000809736	52.6549	0.0169941
20	-7.54952e-14	-7.54952e-14	17.546	3.43551e-05	17.546	5.24152e-05	52.6391	0.00122159
40	1.0747e-13	1.0747e-13	17.546	2.22041e-06	17.546	4.09618e-06	52.638	8.64732e-05
80	1.7033e-12	1.7033e-12	17.546	1.28582e-07	17.546	1.98519e-07	52.6379	4.43784e-06
160	1.94935e-11	1.94935e-11	17.546	8.10197e-09	17.546	1.2524e-08	52.6379	2.83675e-07

(a) P2 conforming on $\hat{\Omega}$

# N	$\hat{\lambda}_{h,1}$	$\hat{\lambda}_{h,1} - \lambda_1$	$\hat{\lambda}_{h,2}$	$\hat{\lambda}_{h,2} - \lambda_2$	$\hat{\lambda}_{h,3}$	$\hat{\lambda}_{h,3} - \lambda_3$	$\hat{\lambda}_{h,4}$	$\hat{\lambda}_{h,4} - \lambda_4$
10	-3.55271e-15	-3.55271e-15	17.5465	0.000553948	17.5466	0.000639161	52.6541	0.0162166
20	9.99201e-15	9.99201e-15	17.546	3.40404e-05	17.546	3.59653e-05	52.6389	0.00100941
40	4.87388e-13	4.87388e-13	17.546	2.28778e-06	17.546	2.37423e-06	52.638	6.55858e-05
80	3.67484e-12	3.67484e-12	17.546	1.32224e-07	17.546	1.35858e-07	52.6379	3.86185e-06
160	3.80063e-11	3.80063e-11	17.546	8.36219e-09	17.546	8.43746e-09	52.6379	2.347e-07

(b) P2 conforming on Ω

Table 2: Eigenvalues using P2 conforming elements on Equilateral

# N	$\hat{\lambda}_{h,1}$	$\hat{\lambda}_{h,1} - \lambda_1$	$\hat{\lambda}_{h,2}$	$\hat{\lambda}_{h,2} - \lambda_2$	$\hat{\lambda}_{h,3}$	$\hat{\lambda}_{h,3} - \lambda_3$	$\hat{\lambda}_{h,4}$	$\hat{\lambda}_{h,4} - \lambda_4$
10	-8.85958e-14	-8.85958e-14	17.546	1.00137e-06	17.546	1.54434e-06	52.638	0.000102184
20	4.52527e-13	4.52527e-13	17.546	1.64527e-08	17.546	2.69642e-08	52.6379	1.72224e-06
40	1.62892e-12	1.62892e-12	17.546	2.91767e-10	17.546	5.00705e-10	52.6379	3.37526e-08
80	1.49671e-11	1.49671e-11	17.546	1.31273e-11	17.546	4.48352e-11	52.6379	4.32813e-10

(a) P3 conforming on $\hat{\Omega}$

# N	$\hat{\lambda}_{h,1}$	$\hat{\lambda}_{h,1} - \lambda_1$	$\hat{\lambda}_{h,2}$	$\hat{\lambda}_{h,2} - \lambda_2$	$\hat{\lambda}_{h,3}$	$\hat{\lambda}_{h,3} - \lambda_3$	$\hat{\lambda}_{h,4}$	$\hat{\lambda}_{h,4} - \lambda_4$
10	-1.42109e-14	-1.42109e-14	17.546	1.07809e-06	17.546	1.16049e-06	52.638	8.70667e-05
20	3.18412e-13	3.18412e-13	17.546	1.64781e-08	17.546	1.72478e-08	52.6379	1.28342e-06
40	1.56852e-12	1.56852e-12	17.546	2.73221e-10	17.546	2.85208e-10	52.6379	2.15863e-08
80	2.35794e-11	2.35794e-11	17.546	2.43752e-11	17.546	4.31086e-11	52.6379	3.2815e-10

(b) P3 conforming on Ω

Table 3: Eigenvalues using P3 conforming elements on Equilateral

# N	$(M_1\nabla\hat{w}_2, \nabla\hat{w}_2)$ $-\hat{\lambda}_{h,2}(\hat{w}_2, \hat{w}_2)$	$(M_1\nabla\hat{w}_3, \nabla\hat{w}_3)$ $-\hat{\lambda}_{h,3}(\hat{w}_3, \hat{w}_3)$	$\int_{\hat{\Omega}} \hat{w}_2\hat{w}_3$	$(M_1\nabla\hat{w}_2, \nabla\hat{w}_2)$ $-\lambda_2(\hat{w}_2, \hat{w}_2)$
10	-5.74887e-15	7.95371e-16	6.68411e-17	0.119482
20	2.03793e-13	2.27637e-14	3.45996e-16	0.0287707
40	1.45394e-13	-4.70743e-14	-4.59505e-16	0.00752098
80	-1.70806e-13	-9.54814e-14	1.36577e-15	0.00180012
160	-6.97301e-13	-2.52874e-12	-6.89345e-17	0.000458361
320	-6.78988e-12	-3.12468e-11	-5.21393e-15	0.000118019

(a) Residuals using P1 conforming on $\hat{\Omega}$

# N	$(M_1\nabla\hat{w}_2, \nabla\hat{w}_2)$ $-\hat{\lambda}_{h,2}(\hat{w}_2, \hat{w}_2)$	$(M_1\nabla\hat{w}_3, \nabla\hat{w}_3)$ $-\hat{\lambda}_{h,3}(\hat{w}_3, \hat{w}_3)$	$\int_{\hat{\Omega}} \hat{w}_2\hat{w}_3$	$(M_1\nabla\hat{w}_2, \nabla\hat{w}_2)$ $-\lambda_2(\hat{w}_2, \hat{w}_2)$
10	-1.41449e-14	-1.19162e-14	-2.1218e-16	0.000279045
20	-3.15712e-13	-1.00704e-14	2.97654e-16	1.93248e-05
40	3.47578e-13	3.95253e-14	7.94137e-16	1.24898e-06
80	-4.45436e-13	-2.27278e-12	1.70018e-15	7.2327e-08
160	-5.30467e-12	-2.91166e-11	-3.12175e-15	4.55205e-09

(b) Residuals using P2 conforming on $\hat{\Omega}$

# N	$(M_1\nabla\hat{w}_2, \nabla\hat{w}_2)$ $-\hat{\lambda}_{h,2}(\hat{w}_2, \hat{w}_2)$	$(M_1\nabla\hat{w}_3, \nabla\hat{w}_3)$ $-\hat{\lambda}_{h,3}(\hat{w}_3, \hat{w}_3)$	$\int_{\hat{\Omega}} \hat{w}_2\hat{w}_3$	$(M_1\nabla\hat{w}_2, \nabla\hat{w}_2)$ $-\lambda_2(\hat{w}_2, \hat{w}_2)$
10	3.43857e-14	6.20354e-14	-5.84987e-17	5.63272e-07
20	-1.04076e-13	-1.38057e-13	1.11831e-15	9.25456e-09
40	5.25742e-12	-2.25444e-12	4.02246e-16	1.69359e-10
80	-5.23658e-12	-2.18083e-11	-2.53596e-15	2.15534e-12

(c) Residuals using P3 conforming on $\hat{\Omega}$

Table 4: Residuals on equilateral triangle

In Tables 1-reftable5e the leftmost column is the number of nodes, N, on one side of the acute triangle. As N increases we expect the computed solutions to be better and better approximations of the true solution. In Table 1 a and b, we compare the use of P1-conforming elements for the isospectral problems (EVP1) and (EVP2). We see that the first three non-zero computed eigenvalues converge, as N increases, to the true solution. The error between the computed and exact eigenvalue decreases roughly by a factor of 4 as we double N. This is the expected quadratic convergence. In the last column of Table 4a, we show the error $\| \int_{\hat{\Omega}} M_1 \nabla \hat{w} \cdot \nabla \hat{w}\, dV - \lambda_2 \int_{\hat{\Omega}} \hat{w}\hat{w}\, dV$; this measures how far the computed eigenfunction is from being the true minimizer of the Ritz quotient. This error decreases quadratically in N.Table **??** c and d, we see the behaviour of P1 non-conforming elements for the isospectral problems (EVP1) and (EVP2). We use the Crouzeix-Raviert elements. Again, we see quadratic convergence of the eigenvalues. Notice that these eigenvalue approximations are lower bounds on the true eigenvalues, as predicted.

In Table 2, we see the behaviour of P2-conforming elements for the isospectral problems (EVP1) and (EVP2). Again, the first three non-zero computed eigenvalues converge, as N increases, to the true solution. The error between the computed and exact eigenvalue decreases roughly by a factor of 16 as we double N. This is the expected quartic convergence. In the last column of Table 4b, we show the error $\| \int_{\hat{\Omega}} M_1 \nabla \hat{w} \cdot \nabla \hat{w}\, dV - \lambda_2 \int_{\hat{\Omega}} \hat{w}\hat{w}\, dV$. This error decreases quartically in N.

In Table 3, we see the behaviour of P2-conforming elements for the isospectral problems (EVP1) and (EVP2). Again, the first three non-zero computed eigenvalues converge, as N increases, to the true solution. The error between the computed and exact eigenvalue initially decreases roughly by a factor of 64 as we double N, but then this levels off. This suggests we should not use cubic polynomials on very refined grids for this problem.

4.1.2 Experiment 2: Isoceles-right triangle

We have a right angled isoceles triangle, with a hypotenuse (PQ) of length 1. Computed coordinates of R= $a_1 = 0.5, b_1 = 0.5$ On this triangle, the first non-zero Neumann eigenvalue is $2\pi^2$.

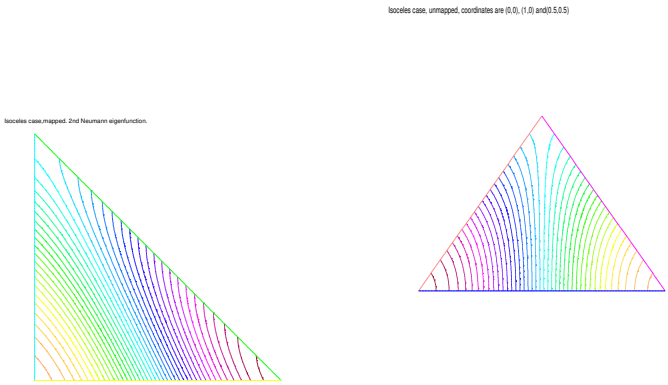

Figure 6: L: 2nd eigenfunction of EVP2 corresponding to isoceles triangle. R: 2nd eigenfunction of EVP1 on isoceles triangle

Similar to the previous section, the figures in the middle rows of 3 and 4 show, graphically, some results for the experiments on the isoceles triangle. In the left plot of Figure 3b, we plot the error $|\lambda_{2,h} - \lambda_2|$ in the computed 2nd Neumann eigenvalue λ_2, for several different methods. As the number of vertices in our tesselation of the domain increases, the mesh size h decreases. From the figure we see clearly that using P1 finite element strategies yields second order convergence for the eigenvalue, while the eigenvalues computed with the P2 conforming strategy converge at 4th order. Also visible here is the behaviour of the P3 (cubic conforming)- the error initially appears to decrease as the number of vertices decreases, but increases again. This is consistent with the theoretical predictions of the behaviour of this method.

In the right graph of figure 3b, we see the effect of computing the 2nd second eigenvalue using the

(isospectral problems) (DVP1) and (DVP2). We see that while the error in the computed eigenvalues is larger if we use a FEM method on the reference triangle, the computed eigenvalues still converge to the correct ones at the same rates.

In the left graph of figure 4b, we present the computed eigenvalues on the actual domain PQR as well as the reference domain, using the P1 and P2 conforming methods, and a suitable P1 non-conforming method (Crouzeiux-Raviert elements). One can clearly see that the computed eigenvalues using conforming and this non-conforming method approach the true value from opposite sides. For each mesh size h, one can therefore use the P1 conforming and non-conforming methods to get an interval, within which the true eigenvalue must lie. As h decreases, this interval will become smaller. In the middle and right plots of 4a, we show how close the computed eigenvalues and eigenvectors of the discrete system (8) are to the exact eigenpair for this system. The eigenvalues are simple. We notice both $\frac{\|r\|_{2,h}^2}{\delta}$ and $\frac{\|r\|_2}{\delta}$ behave in a monotone fashion as h decreases. For small enough h, the angle between the computed eigenvector $\tilde{u}$ and the true eigenvector fo the discrete system $\vec{u}$ is within $asin(1e-3)$.

# N	$\hat{\lambda}_{h,1}$	$\hat{\lambda}_{h,1} - \lambda_1$	$\hat{\lambda}_{h,2}$	$\hat{\lambda}_{h,2} - \lambda_2$	$\hat{\lambda}_{h,3}$	$\hat{\lambda}_{h,3} - \lambda_3$	$\hat{\lambda}_{h,4}$	$\hat{\lambda}_{h,4} - \lambda_4$
10	1.86517e-14	1.86517e-14	19.9666	0.227403	40.8815	1.40306	82.5674	3.61054
20	6.43929e-15	6.43929e-15	19.8018	0.0626121	39.8095	0.331124	79.8766	0.919792
40	9.88098e-14	9.88098e-14	19.7565	0.0172549	39.5779	0.0994429	79.2276	0.270728
80	-8.46878e-13	-8.46878e-13	19.7433	0.00405659	39.501	0.0225744	79.0189	0.0620967
160	7.49356e-12	7.49356e-12	19.7402	0.00102338	39.4842	0.00573398	78.9724	0.0155909
320	5.27827e-11	5.27827e-11	19.7395	0.000264352	39.4799	0.00150088	78.9609	0.00406253

(a) P1 conforming on $\hat{\Omega}$

# N	$\hat{\lambda}_{h,1}$	$\hat{\lambda}_{h,1} - \lambda_1$	$\hat{\lambda}_{h,2}$	$\hat{\lambda}_{h,2} - \lambda_2$	$\hat{\lambda}_{h,3}$	$\hat{\lambda}_{h,3} - \lambda_3$	$\hat{\lambda}_{h,4}$	$\hat{\lambda}_{h,4} - \lambda_4$
10	2.37588e-14	2.37588e-14	19.8999	0.160678	40.2722	0.793785	81.7947	2.83789
20	-1.86517e-14	-1.86517e-14	19.7833	0.0440767	39.6982	0.219746	79.6972	0.740349
40	-1.09468e-13	-1.09468e-13	19.751	0.0118294	39.533	0.0545847	79.1534	0.196527
80	6.48148e-13	6.48148e-13	19.7421	0.00286415	39.4922	0.0137468	79.0053	0.0484561
160	4.4873e-12	4.4873e-12	19.7399	0.000719624	39.4818	0.00342958	78.9689	0.0120712
320	3.42069e-11	3.42069e-11	19.7394	0.000173133	39.4793	0.000841499	78.9598	0.00298509

(b) P1 conforming on Ω

# N	$\hat{\lambda}_{h,1}$	$\hat{\lambda}_{h,1} - \lambda_1$	$\hat{\lambda}_{h,2}$	$\hat{\lambda}_{h,2} - \lambda_2$	$\hat{\lambda}_{h,3}$	$\hat{\lambda}_{h,3} - \lambda_3$	$\hat{\lambda}_{h,4}$	$\hat{\lambda}_{h,4} - \lambda_4$
10	4.06342e-14	4.06342e-14	19.4679	-0.271272	39.0984	-0.379996	74.1591	-4.79771
20	5.90639e-14	5.90639e-14	19.6746	-0.0645679	39.404	-0.0744489	77.6998	-1.25699
40	5.20251e-13	5.20251e-13	19.7212	-0.0180446	39.454	-0.0243718	78.6654	-0.291457
80	2.60636e-12	2.60636e-12	19.7347	-0.00451666	39.4722	-0.00624669	78.8837	-0.0731796
160	3.24212e-11	3.24212e-11	19.7381	-0.00112518	39.4769	-0.00149391	78.9385	-0.0182884
320	1.9995e-10	1.9995e-10	19.7389	-0.00026751	39.4781	-0.000304342	78.9522	-0.00466608

(c) P1 nonconforming on $\hat{\Omega}$

# N	$\hat{\lambda}_{h,1}$	$\hat{\lambda}_{h,1} - \lambda_1$	$\hat{\lambda}_{h,2}$	$\hat{\lambda}_{h,2} - \lambda_2$	$\hat{\lambda}_{h,3}$	$\hat{\lambda}_{h,3} - \lambda_3$	$\hat{\lambda}_{h,4}$	$\hat{\lambda}_{h,4} - \lambda_4$
10	-1.79856e-14	-1.79856e-14	19.7008	-0.0384408	39.0914	-0.387055	78.2588	-0.698048
20	-9.32587e-14	-9.32587e-14	19.7285	-0.0106652	39.3825	-0.0959036	78.7371	-0.219782
40	-1.96732e-13	-1.96732e-13	19.7362	-0.00298979	39.4521	-0.0262916	78.904	-0.0528608
80	1.17373e-12	1.17373e-12	19.7386	-0.00061972	39.4719	-0.00656222	78.9438	-0.0130143
160	2.22138e-11	2.22138e-11	19.7391	-0.000158499	39.4768	-0.00162765	78.9536	-0.00324469
320	2.49265e-10	2.49265e-10	19.7392	-3.74717e-05	39.478	-0.000398592	78.9561	-0.000760053

(d) P1 nonconforming on Ω

Table 5: Eigenvalues using P1 conforming elements on Isoceles

# N	$\hat{\lambda}_{h,1}$	$\hat{\lambda}_{h,1} - \lambda_1$	$\hat{\lambda}_{h,2}$	$\hat{\lambda}_{h,2} - \lambda_2$	$\hat{\lambda}_{h,3}$	$\hat{\lambda}_{h,3} - \lambda_3$	$\hat{\lambda}_{h,4}$	$\hat{\lambda}_{h,4} - \lambda_4$
10	9.08162e-14	9.08162e-14	19.7398	0.000634195	39.4871	0.00870996	78.99	0.0331314
20	-3.21965e-13	-3.21965e-13	19.7392	4.03215e-05	39.479	0.000538308	78.9593	0.00248306
40	1.06803e-13	1.06803e-13	19.7392	3.354e-06	39.4785	4.06787e-05	78.957	0.000192829
80	6.39755e-12	6.39755e-12	19.7392	1.61827e-07	39.4784	2.37126e-06	78.9568	9.22855e-06
160	8.13272e-11	8.13272e-11	19.7392	1.03115e-08	39.4784	1.46595e-07	78.9568	5.88372e-07

(a) P2 conforming on $\hat{\Omega}$

# N	$\hat{\lambda}_{h,1}$	$\hat{\lambda}_{h,1} - \lambda_1$	$\hat{\lambda}_{h,2}$	$\hat{\lambda}_{h,2} - \lambda_2$	$\hat{\lambda}_{h,3}$	$\hat{\lambda}_{h,3} - \lambda_3$	$\hat{\lambda}_{h,4}$	$\hat{\lambda}_{h,4} - \lambda_4$
10	-4.37428e-14	-4.37428e-14	19.7396	0.000398967	39.4807	0.00229702	78.9801	0.0232553
20	1.18572e-13	1.18572e-13	19.7392	3.00767e-05	39.4786	0.00018957	78.9586	0.00180742
40	1.71196e-13	1.71196e-13	19.7392	1.89651e-06	39.4784	1.23327e-05	78.9569	0.000112854
80	4.48419e-12	4.48419e-12	19.7392	1.21081e-07	39.4784	7.61106e-07	78.9568	7.01324e-06
160	5.55431e-11	5.55431e-11	19.7392	7.53363e-09	39.4784	4.80816e-08	78.9568	4.36602e-07

(b) P2 conforming on Ω

Table 6: Eigenvalues using P2 conforming elements on Isoceles

# N	$\hat{\lambda}_{h,1}$	$\hat{\lambda}_{h,1} - \lambda_1$	$\hat{\lambda}_{h,2}$	$\hat{\lambda}_{h,2} - \lambda_2$	$\hat{\lambda}_{h,3}$	$\hat{\lambda}_{h,3} - \lambda_3$	$\hat{\lambda}_{h,4}$	$\hat{\lambda}_{h,4} - \lambda_4$
10	8.88178e-15	8.88178e-15	19.7392	9.37997e-07	39.4784	3.14511e-05	78.957	0.000209274
20	4.49196e-13	4.49196e-13	19.7392	1.66245e-08	39.4784	4.89056e-07	78.9568	3.52566e-06
40	3.95972e-12	3.95972e-12	19.7392	3.31344e-10	39.4784	1.02019e-08	78.9568	7.4787e-08
80	2.49756e-11	2.49756e-11	19.7392	4.36806e-11	39.4784	1.60789e-10	78.9568	9.0975e-10

(a) P3 conforming on $\hat{\Omega}$

# N	$\hat{\lambda}_{h,1}$	$\hat{\lambda}_{h,1} - \lambda_1$	$\hat{\lambda}_{h,2}$	$\hat{\lambda}_{h,2} - \lambda_2$	$\hat{\lambda}_{h,3}$	$\hat{\lambda}_{h,3} - \lambda_3$	$\hat{\lambda}_{h,4}$	$\hat{\lambda}_{h,4} - \lambda_4$
10	1.33227e-14	1.33227e-14	19.7392	4.88056e-07	39.4784	8.50386e-06	78.957	0.000121503
20	6.00187e-13	6.00187e-13	19.7392	1.00951e-08	39.4784	1.74254e-07	78.9568	2.60624e-06
40	2.67519e-12	2.67519e-12	19.7392	1.6983e-10	39.4784	2.78617e-09	78.9568	4.32339e-08
80	3.4124e-11	3.4124e-11	19.7392	2.58424e-11	39.4784	9.96323e-11	78.9568	7.22821e-10

(b) P3 conforming on Ω

Table 7: Eigenvalues using P3 conforming elements on Isoceles

# N	$(M_1\nabla\hat{w}_2, \nabla\hat{w}_2)$ $-\hat{\lambda}_{h,2}(\hat{w}_2, \hat{w}_2)$	$(M_1\nabla\hat{w}_3, \nabla\hat{w}_3)$ $-\hat{\lambda}_{h,3}(\hat{w}_3, \hat{w}_3)$	$\int_{\hat{\Omega}} \hat{w}_2\hat{w}_3$	$(M_1\nabla\hat{w}_2, \nabla\hat{w}_2)$ $-\lambda_2(\hat{w}_2, \hat{w}_2)$
10	-3.11632e-15	-2.18272e-15	-1.89193e-17	0.0142127
20	-1.48265e-16	5.30934e-15	5.29048e-17	0.00391326
40	7.72499e-15	1.11248e-14	1.5221e-16	0.00107843
80	3.76742e-14	5.14823e-15	1.00916e-16	0.000253537
160	-9.79429e-13	-6.19048e-13	2.91677e-16	6.39614e-05
320	-5.93016e-12	-5.71244e-12	-7.15207e-16	1.6522e-05

(a) Residuals using P1 conforming on $\hat{\Omega}$

# N	$(M_1\nabla\hat{w}_2, \nabla\hat{w}_2)$ $-\hat{\lambda}_{h,2}(\hat{w}_2, \hat{w}_2)$	$(M_1\nabla\hat{w}_3, \nabla\hat{w}_3)$ $-\hat{\lambda}_{h,3}(\hat{w}_3, \hat{w}_3)$	$\int_{\hat{\Omega}} \hat{w}_2\hat{w}_3$	$(M_1\nabla\hat{w}_2, \nabla\hat{w}_2)$ $-\lambda_2(\hat{w}_2, \hat{w}_2)$
10	-3.75481e-15	-2.94296e-15	-5.61075e-18	3.96372e-05
20	4.53197e-15	2.02633e-14	1.33836e-16	2.5201e-06
40	3.10755e-14	7.69556e-15	6.98362e-17	2.09625e-07
80	-7.8333e-13	-7.34698e-13	1.31699e-16	1.01134e-08
160	-9.36753e-12	-5.78586e-12	-2.03855e-15	6.35106e-10

(b) Residuals using P2 conforming on $\hat{\Omega}$

# N	$(M_1\nabla\hat{w}_2, \nabla\hat{w}_2)$ $-\hat{\lambda}_{h,2}(\hat{w}_2, \hat{w}_2)$	$(M_1\nabla\hat{w}_3, \nabla\hat{w}_3)$ $-\hat{\lambda}_{h,3}(\hat{w}_3, \hat{w}_3)$	$\int_{\hat{\Omega}} \hat{w}_2\hat{w}_3$	$(M_1\nabla\hat{w}_2, \nabla\hat{w}_2)$ $-\lambda_2(\hat{w}_2, \hat{w}_2)$
10	-1.25703e-14	1.87099e-14	1.42722e-16	5.86248e-08
20	-3.15012e-14	-2.82738e-15	-1.72859e-16	1.039e-09
40	-4.91417e-13	-3.41933e-13	8.60247e-17	2.02175e-11
80	-2.48994e-12	-2.58628e-12	-7.34202e-16	2.44128e-13

(c) Residuals using P3 conforming on $\hat{\Omega}$

Table 8: Residuals on Isoceles triangle

4.1.3 Experiment 3: 40-60-80 triangle

We consider a triangle with 40-60-80 degree angles. We no longer have analytical expressions for the eigenvalues. Instead, we first compute the eigenvalues using P2-conforming finite elements on the original domain PQR for a very refined grid, and use this as our 'true' eigenvalue guess. We obtain $\lambda_1 = 0, \lambda_2 \approx 17.820219743795281175, \lambda_3 \approx 37.623868539943330802, \lambda_4 \approx 61.846304317214197965$. We record some of the results in the bottom rows of Figures 3 and 4. Since we do not have true eigenvalues, the plots in 3c should be interpreted carefully: these compare the computed eigenvalues to a highly refined calculation. The plots in 4c are a better indication of the quality of the results, since they don't rely on the actual eigenvalues.

# N	$\hat{\lambda}_{h,1}$	$\hat{\lambda}_{h,2}$	$\hat{\lambda}_{h,3}$	$\hat{\lambda}_{h,4}$
10	-9.54792e-15	18.0125	38.5319	64.4134
20	6.77236e-14	17.8679	37.8537	62.4683
40	1.59872e-13	17.8332	37.6863	62.0121
80	-1.59872e-14	17.8234	37.6386	61.8888
160	5.3928e-12	17.821	37.6276	61.8569
320	3.0185e-11	17.8204	37.6248	61.8489

(a) P1 conforming on $\hat{\Omega}$

# N	$\hat{\lambda}_{h,1}$	$\hat{\lambda}_{h,2}$	$\hat{\lambda}_{h,3}$	$\hat{\lambda}_{h,4}$
10	1.62093e-14	17.9895	38.4454	64.1808
20	-7.37188e-14	17.8644	37.8244	62.3928
40	6.72795e-14	17.831	37.6752	61.9832
80	2.57572e-13	17.8229	37.6364	61.8806
160	3.1235e-12	17.8209	37.627	61.8549
320	3.31766e-11	17.8204	37.6246	61.8484

(b) P1 conforming on Ω

Table 9: Eigenvalues using P1 conforming elements on Generic

# N	$\hat{\lambda}_{h,1}$	$\hat{\lambda}_{h,2}$	$\hat{\lambda}_{h,3}$	$\hat{\lambda}_{h,4}$
10	-8.32667e-14	17.8207	37.6282	61.8658
20	-3.05533e-13	17.8202	37.6241	61.8475
40	7.20091e-13	17.8202	37.6239	61.8464
80	1.17728e-12	17.8202	37.6239	61.8463
160	5.77316e-11	17.8202	37.6239	61.8463

(a) P2 conforming on $\hat{\Omega}$

# N	$\hat{\lambda}_{h,1}$	$\hat{\lambda}_{h,2}$	$\hat{\lambda}_{h,3}$	$\hat{\lambda}_{h,4}$
10	-1.14353e-13	17.8207	37.6269	61.8658
20	8.03801e-14	17.8202	37.6241	61.8474
40	2.39808e-13	17.8202	37.6239	61.8464
80	5.62106e-12	17.8202	37.6239	61.8463
160	5.22926e-11	17.8202	37.6239	61.8463

(b) P2 conforming on Ω

Table 10: Eigenvalues using P2 conforming elements on Generic

# N	$\hat{\lambda}_{h,1}$	$\hat{\lambda}_{h,2}$	$\hat{\lambda}_{h,3}$	$\hat{\lambda}_{h,4}$
10	-1.7053e-13	17.8202	37.6239	61.8464
20	-4.35207e-14	17.8202	37.6239	61.8463
40	8.68194e-13	17.8202	37.6239	61.8463
80	1.27212e-11	17.8202	37.6239	61.8463

(a) P3 conforming on $\hat{\Omega}$

# N	$\hat{\lambda}_{h,1}$	$\hat{\lambda}_{h,2}$	$\hat{\lambda}_{h,3}$	$\hat{\lambda}_{h,4}$
10	-1.82965e-13	17.8202	37.6239	61.8464
20	-3.38396e-13	17.8202	37.6239	61.8463
40	2.4869e-12	17.8202	37.6239	61.8463
80	2.64175e-11	17.8202	37.6239	61.8463

(b) P3 conforming on Ω

Table 11: Eigenvalues using P3 conforming elements on Generic

# N	$\hat{\lambda}_{h,1}$	$\hat{\lambda}_{h,2}$	$\hat{\lambda}_{h,3}$	$\hat{\lambda}_{h,4}$
10	-1.42553e-13	17.6841	37.2183	59.6737
20	1.00586e-13	17.7848	37.5385	61.3088
40	1.99618e-13	17.8108	37.5982	61.7198
80	2.48424e-12	17.8179	37.6175	61.8138
160	3.18865e-11	17.8196	37.6223	61.8383
320	1.63209e-10	17.8201	37.6235	61.8443

(a) P1 nonconforming on $\hat{\Omega}$

# N	$\hat{\lambda}_{h,1}$	$\hat{\lambda}_{h,2}$	$\hat{\lambda}_{h,3}$	$\hat{\lambda}_{h,4}$
10	3.4639e-14	17.7669	37.3183	60.9477
20	-1.15463e-13	17.8081	37.5407	61.6662
40	-1.41442e-13	17.8172	37.6015	61.7992
80	2.36811e-12	17.8195	37.6183	61.8344
160	8.51319e-12	17.82	37.6224	61.8433
320	2.03408e-10	17.8202	37.6235	61.8456

(b) P1 nonconforming on Ω

Table 12: Eigenvalues using P1 non-conforming elements on Generic

# N	$(M_1\nabla\hat{w}_2,\nabla\hat{w}_2)$ $-\hat{\lambda}_{h,2}(\hat{w}_2,\hat{w}_2)$	$(M_1\nabla\hat{w}_3,\nabla\hat{w}_3)$ $-\hat{\lambda}_{h,3}(\hat{w}_3,\hat{w}_3)$	$\int_{\hat{\Omega}}\hat{w}_2\hat{w}_3$
10	-3.57657e-15	-1.82341e-15	-7.19233e-17
20	-1.5318e-14	-6.01331e-15	-1.30765e-16
40	-2.46087e-14	-8.98028e-15	-1.01806e-16
80	2.97193e-14	-7.46185e-14	5.11921e-16
160	-6.67034e-13	-7.06641e-13	1.01623e-16
320	-2.74598e-12	-6.05465e-12	-1.91497e-15

(a) Residuals using P1 conforming on $\hat{\Omega}$

# N	$(M_1\nabla\hat{w}_2,\nabla\hat{w}_2)$ $-\hat{\lambda}_{h,2}(\hat{w}_2,\hat{w}_2)$	$(M_1\nabla\hat{w}_3,\nabla\hat{w}_3)$ $-\hat{\lambda}_{h,3}(\hat{w}_3,\hat{w}_3)$	$\int_{\hat{\Omega}}\hat{w}_2\hat{w}_3$
10	2.16624e-15	-3.37902e-15	2.67391e-17
20	-1.91865e-14	3.51891e-14	-3.32613e-17
40	-6.18127e-14	-2.51864e-14	2.41087e-17
80	1.15242e-14	-3.41607e-13	-1.23831e-15
160	-7.77088e-12	-9.0248e-12	-1.02168e-16

(b) Residuals using P2 conforming on $\hat{\Omega}$

# N	$(M_1\nabla\hat{w}_2,\nabla\hat{w}_2)$ $-\hat{\lambda}_{h,2}(\hat{w}_2,\hat{w}_2)$	$(M_1\nabla\hat{w}_3,\nabla\hat{w}_3)$ $-\hat{\lambda}_{h,3}(\hat{w}_3,\hat{w}_3)$	$\int_{\hat{\Omega}}\hat{w}_2\hat{w}_3$
10	3.65511e-14	2.01729e-14	7.62601e-17
20	3.41149e-14	-6.48493e-14	1.64155e-16
40	-1.9376e-13	-2.17753e-13	3.0523e-16
80	-7.24557e-13	-2.82311e-12	-7.94297e-16

(c) Residuals using P3 conforming on $\hat{\Omega}$

Table 13: Residuals on 40-60-80 triangle

5 Results

In this section we present some results. In the first set of graphs 7 - 10, we explore the parameter space where $\frac{\pi}{4} \leq \alpha \leq \frac{\pi}{2}, 0 \leq \beta \leq \frac{\pi}{2}, \alpha + \beta \geq \frac{\pi}{2}, \beta \leq \alpha$. This is a larger region of parameter than we need to explore. However, we use a uniform grid in parameter space to compute the bounds from Section **??**. This will provide an indication of how finely to sample the desired region of parameter space, $\frac{\pi}{4} \leq \alpha \leq \frac{\pi}{2}, 0 \leq \beta \leq \frac{\pi}{3}, \alpha + \beta \geq \frac{\pi}{2}, \beta \leq \alpha$.

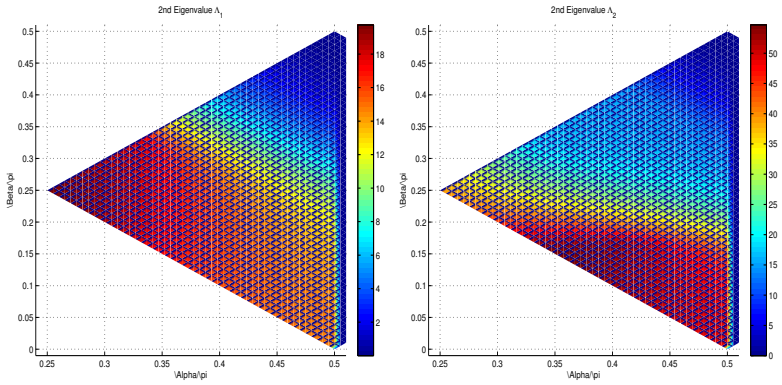

Figure 7: L: 2nd Neumann eigenvalue as a function of $\frac{1}{\pi}(\alpha, \beta)$. R:3rd Neumann eigenvalue as a function of $\frac{1}{\pi}(\alpha, \beta)$

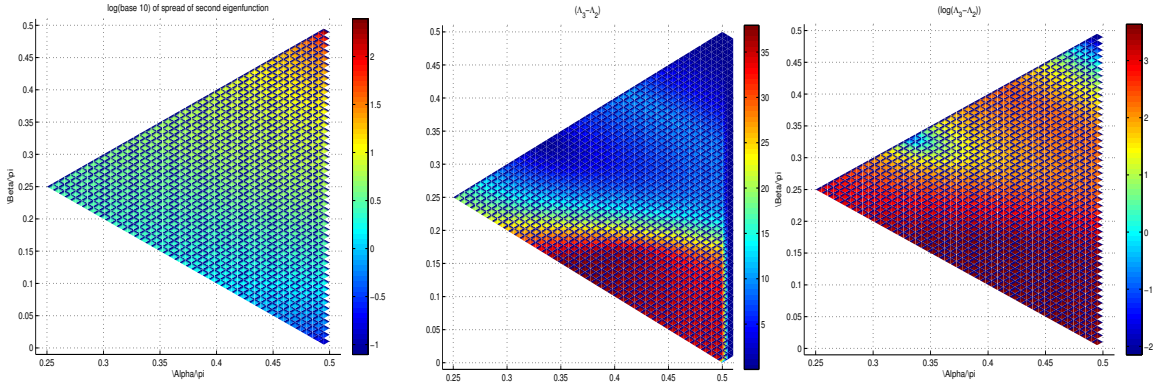

Figure 8: L: $log_{10}|u_{max} - u_{min}|$ for the second Neumann eigenfunction, as a function of $\frac{1}{\pi}(\alpha, \beta)$. M: Spectral gap $\lambda_3 - \lambda_2$ as a function of $\frac{1}{\pi}(\alpha, \beta)$. R: $\ln|\lambda_3 - \lambda_2|$

Using the grid sizing from Figure9 as a guide, the region $\frac{\pi}{4} \leq \alpha \leq \frac{\pi}{2}, 0 \leq \beta \leq \frac{\pi}{3}, \alpha + \beta \geq \frac{\pi}{2}, \beta \leq \alpha$ was sampled at discrete points. At each of these points, the algorithm to numerically verify the Hot Spot conjecture was run. Computations were performed (a) using Matlab codes based on programs written by Joseph Coyle, (only conforming methods) and (b) using FreeFem++ (conforming and P1-non-conforming methods).

For each of the points sampled, the Hot Spot conjecture was verified. The extrema of the computed eigenfunction lies at a corner of the triagle PQR in each instance.

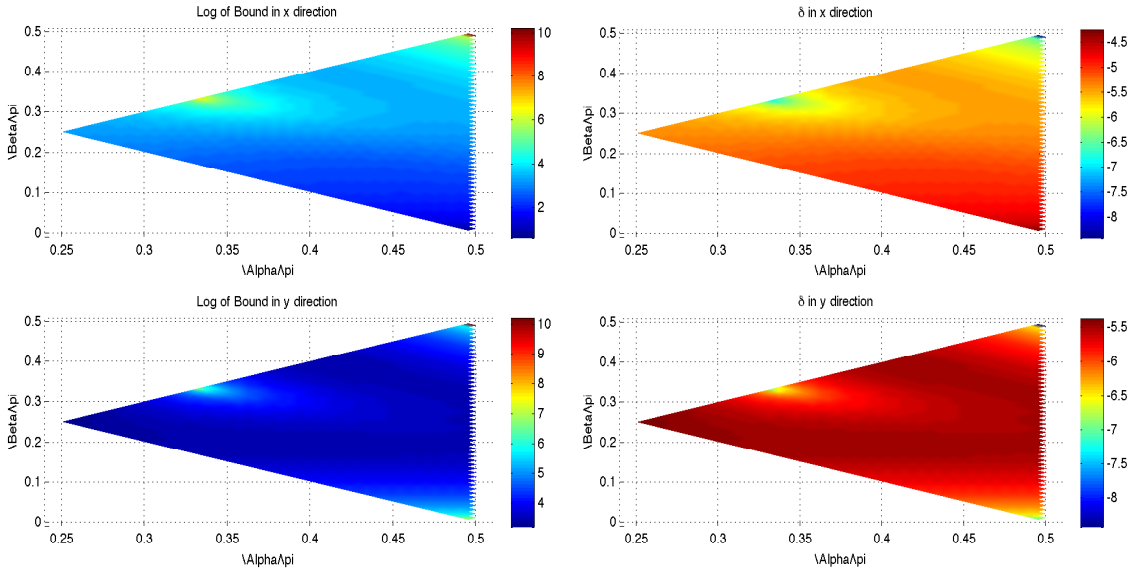

Figure 9: L: Log of bounds, ref. Section3. R: Grid sizing to ensure tolerance of 1e-4. $\log_{10}(\delta)$ in x and y direction

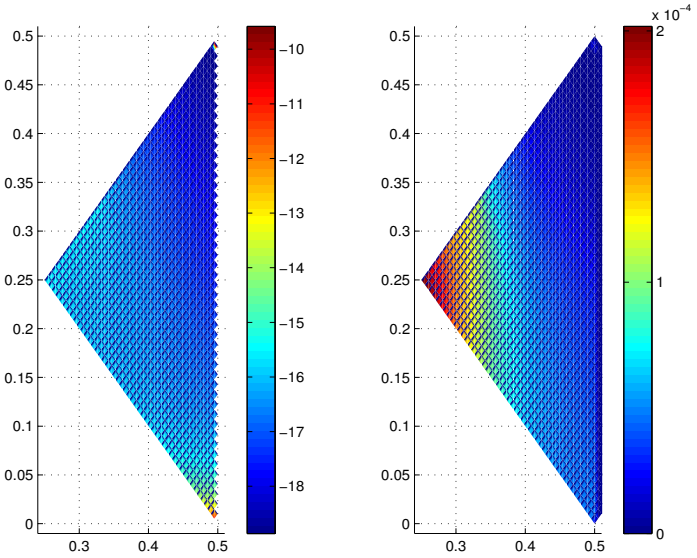

Figure 10: L: $\ln|\lambda_{2,h_n} - \lambda_{2,h_{n+1}}|$ using P2 conforming on successive grids. R: $|\lambda_{2,P2} - \lambda_{2,P1nc}|$ using P2 conforming and P1 non-conforming

References

[1] María G. Armentano and Ricardo G. Durán. Asymptotic lower bounds for eigenvalues by nonconforming finite element methods. *Electron. Trans. Numer. Anal.*, 17:93–101 (electronic), 2004.

[2] I. Babuška and J. Osborn. Eigenvalue problems. In *Handbook of numerical analysis, Vol. II*, Handb. Numer. Anal., II, pages 641–787. North-Holland, Amsterdam, 1991.

[3] Philippe G. Ciarlet. *The finite element method for elliptic problems*, volume 40 of *Classics in Applied Mathematics*. Society for Industrial and Applied Mathematics (SIAM), Philadelphia, PA, 2002. Reprint of the 1978 original [North-Holland, Amsterdam; MR0520174 (58 #25001)].

[4] Gene H. Golub and Charles F. Van Loan. *Matrix computations*. Johns Hopkins Studies in the Mathematical Sciences. Johns Hopkins University Press, Baltimore, MD, third edition, 1996.

[5] Brian J. McCartin. Eigenstructure of the equilateral triangle. II. The Neumann problem. *Math. Probl. Eng.*, 8(6):517–539, 2002.

[6] C. C. Paige. Error analysis of the Lanczos algorithm for tridiagonalizing a symmetric matrix. *J. Inst. Math. Appl.*, 18(3):341–349, 1976.

[7] C. C. Paige. Accuracy and effectiveness of the Lanczos algorithm for the symmetric eigenproblem. *Linear Algebra Appl.*, 34:235–258, 1980.

[8] Rolf Rannacher and Ridgway Scott. Some optimal error estimates for piecewise linear finite element approximations. *Math. Comp.*, 38(158):437–445, 1982.

[9] Lloyd N. Trefethen and David Bau, III. *Numerical linear algebra*. Society for Industrial and Applied Mathematics (SIAM), Philadelphia, PA, 1997.

[10] Olof Widlund. On best error bounds for approximation by piecewise polynomial functions. *Numer. Math.*, 27(3):327–338, 1976/77.

[11] YiDu Yang, ZhiMin Zhang, and FuBiao Lin. Eigenvalue approximation from below using non-conforming finite elements. *Sci. China Math.*, 53(1):137–150, 2010.